

# Symbolic Music Generation with Diffusion Models

Gautam Mittal<sup>1\*</sup> Jesse Engel<sup>2</sup> Curtis Hawthorne<sup>2</sup> Ian Simon<sup>2</sup>

## Abstract

Score-based generative models and diffusion probabilistic models have been successful at generating high-quality samples in continuous domains such as images and audio. However, due to their Langevin-inspired sampling mechanisms, their application to discrete and sequential data has been limited. In this work, we present a technique for training diffusion models on sequential data by parameterizing the discrete domain in the continuous latent space of a pre-trained variational autoencoder. Our method is non-autoregressive and learns to generate sequences of latent embeddings through the reverse process and offers parallel generation with a constant number of iterative refinement steps. We apply this technique to modeling symbolic music and show strong unconditional generation and post-hoc conditional infilling results compared to autoregressive language models operating over the same continuous embeddings.

## 1. Introduction

Recent progress in deep generative modeling has led to many advances in representing both discrete and continuous domains. Variational autoencoders (VAEs) (Kingma & Welling, 2014), generative adversarial networks (GANs) (Goodfellow et al., 2014), and autoregressive models (ARs) (Oord et al., 2016) have been able to generate high-quality image, audio, and text samples that accurately mirror data distributions.

In the music domain, these techniques have led to improvements in expressive unconditional and conditional generation of both continuous audio (Engel et al., 2017b; 2019; Dhariwal et al., 2020; Engel et al., 2020), and discrete symbolic music (Huang et al., 2017; 2018; Simon et al., 2018; Payne, 2019; Dinculescu et al., 2019; Donahue et al., 2019; Wang et al., 2020; Choi et al., 2020; Huang & Yang, 2020).

<sup>1</sup>Department of EECS, University of California, Berkeley, Berkeley, California, USA <sup>\*</sup>Work completed during an internship at Google Brain <sup>2</sup>Google Brain, Mountain View, California, USA. Correspondence to: Gautam Mittal <gbm@berkeley.edu>.

Denoising diffusion probabilistic models (DDPMs) (Sohl-Dickstein et al., 2015; Ho et al., 2020) are a promising new class of generative models that can generate comparably high-quality samples (Chen et al., 2020; Kong et al., 2020) by learning to invert a diffusion process from data to Gaussian noise. Unlike other deep generative models, DDPMs sample through an iterative refinement process inspired by Langevin dynamics, which enables post-hoc conditioning of models trained unconditionally (Song & Ermon, 2019; 2020; Du & Mordatch, 2020) that enables creative opportunities in applications such as music (Engel et al., 2017a).

Iterative refinement, however, operates on continuous data, which has restricted DDPMs to domains such as images and audio, and prevented applying them to discrete data such as text and symbolic music. Similarly, DDPMs cannot take advantage of the recent advances in modeling long-term structure (Razavi et al., 2019; Dhariwal et al., 2020; Ramesh et al., 2021) that use a two-stage process of modeling discrete tokens extracted by a separate low-level autoencoder.

In this paper, we demonstrate that it is possible to overcome these limitations by training DDPMs on the continuous latents of low-level VAEs to generate long-form discrete symbolic music. Our key findings include:

- High-quality unconditional sampling of discrete melodic sequences (up to length 1024) with DDPMs through iterative refinement of lower-level VAE latents.
- DDPMs outperforming strong AR baselines (TransformerMDN) in hierarchical modeling of continuous latents, partly due to a lack of teacher forcing and exposure bias during training.
- A method to identify and remove underused dimensions in VAE latents, crucial for hierarchical modeling both with DDPMs and AR models.
- Post-hoc conditional infilling of melodic sequences for creative applications.

## 2. Background

### 2.1. Denoising Diffusion Probabilistic Models (DDPMs)

DDPMs (Sohl-Dickstein et al., 2015; Ho et al., 2020) are a class of generative models that define latents  $x_1, \dots, x_N$  of

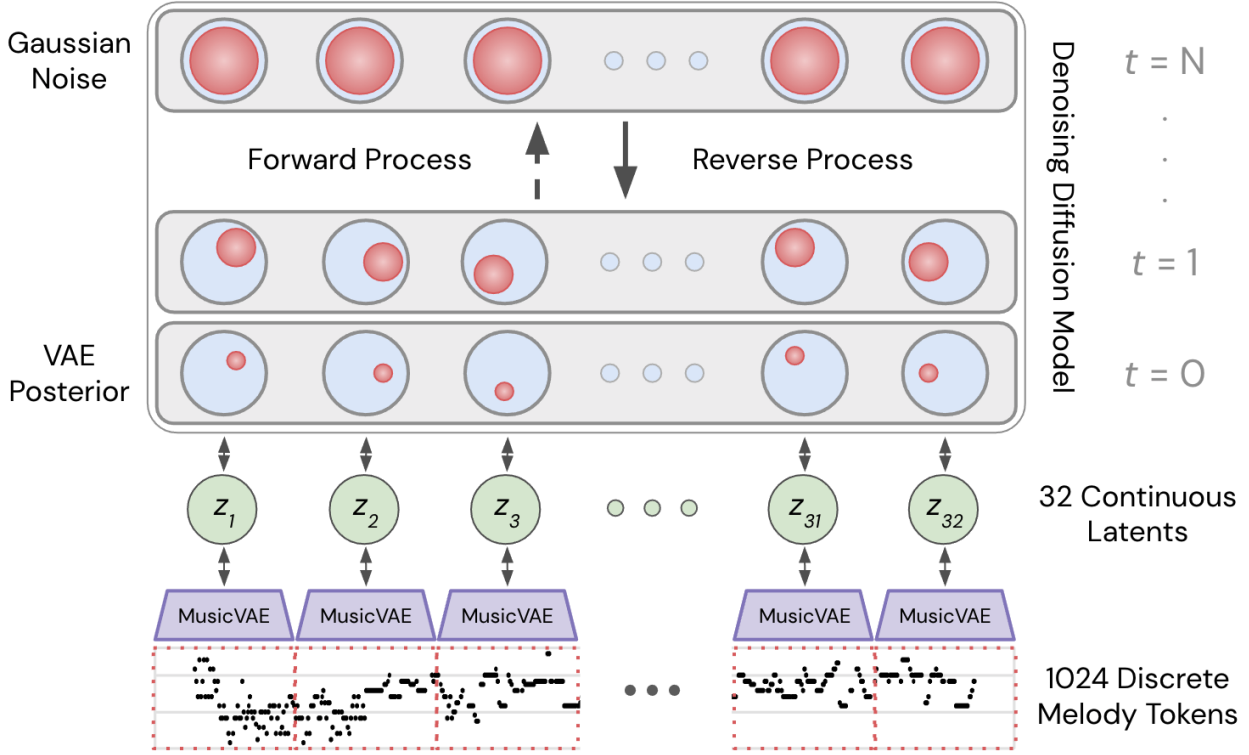


Figure 1. A diagram of our proposed framework. We use the pre-trained 2-bar melody MusicVAE (Roberts et al., 2019) to embed discrete musical phrases (64 bars, 1024 tokens) into a sequence of continuous latent codes (32 latents, 512 dimensions each). These embeddings are used to train a diffusion model that iteratively adds noise such that after  $N$  diffusion steps the input embeddings are distributed  $\mathcal{N}(0, I)$ . To sample from this model, we initialize Gaussian noise and use the reverse process to iteratively refine the noise samples into a sequence of embeddings from the data distribution. These generated embeddings are fed through the MusicVAE decoder to produce the final MIDI sequence.

the same dimensionality as the data  $x_0 \sim q(x_0)$ . For brevity, we refer to these models as diffusion models. Diffusion models are comprised of a **forward process** and a **reverse process**. The **forward process** starts from the data  $x_0$  and iteratively adds Gaussian noise according to a fixed noise schedule for  $N$  diffusion steps:

$$q(x_t|x_{t-1}) = \mathcal{N}(x_t; \sqrt{1 - \beta_t}x_{t-1}, \beta_t I) \quad (1)$$

$$q(x_{1:N}|x_0) = \prod_{t=1}^N q(x_t|x_{t-1}) \quad (2)$$

where  $\beta_1, \beta_2, \dots, \beta_N$  is a noise schedule that converts the data distribution  $x_0$  into latent  $x_N$ . The choice of noise schedule has been shown to have important effects on sampling efficiency and quality (Chen et al., 2020; Ho et al., 2020).

The **reverse process** is defined by a Markov chain parameterized by  $\theta$  that iteratively refines latent point  $x_N \sim \mathcal{N}(0, I)$  into data point  $x_0$ . The learned transition probabilities are defined as,

$$p_\theta(x_{t-1}|x_t) = \mathcal{N}(x_{t-1}; \mu_\theta(x_t, t), \sigma_\theta(x_t, t)) \quad (3)$$

$$p_\theta(x_{0:N}) = p(x_N) \prod_{t=1}^N p_\theta(x_{t-1}|x_t) \quad (4)$$

where the objective is to gradually denoise samples at each reverse diffusion step  $t$ . In practice,  $\sigma_\theta$  is set to an untrained time-dependent constant based on the noise schedule, and Ho et al. (2020) found  $\sigma_\theta(x_t, t) = \sigma_t = \frac{1 - \bar{\alpha}_{t-1}}{1 - \bar{\alpha}_t} \beta_t$  to have reasonable experimental results, where  $\alpha_t = 1 - \beta_t$ , and  $\bar{\alpha}_t = \prod_{i=1}^t \alpha_i$ .

The training objective is to maximize the log likelihood of  $p_\theta(x_0) = \int p_\theta(x_0, \dots, x_N) dx_{1:N}$ , but the intractability of this marginalization leads to the following evidence lower bound (ELBO):

$$\begin{aligned} \mathbb{E}[\log p_\theta(x_0)] &\geq \mathbb{E}_q \left[ \log \frac{p_\theta(x_{0:N})}{q(x_{1:N}|x_0)} \right] \\ &= \mathbb{E}_q \left[ \log p(x_N) + \sum_{t \geq 1} \log \frac{p_\theta(x_{t-1}|x_t)}{q(x_t|x_{t-1})} \right] \end{aligned} \quad (5)$$

**Algorithm 1** Training

---

**Input:**  $q(x_0)$ ,  $N$  steps, noise schedule  $\beta_1, \dots, \beta_N$   
**repeat**  
 $x_0 \sim q(x_0)$   
 $t \sim \mathbb{U}(\{1, \dots, N\})$   
 $\sqrt{\alpha} \sim \mathbb{U}(\sqrt{\alpha_{t-1}}, \sqrt{\alpha_t})$   
 $\epsilon \sim \mathcal{N}(0, I)$   
 Take gradient descent step on  
 $\nabla_{\theta} \|\epsilon - \epsilon_{\theta}(\sqrt{\alpha_t}x_0 + \sqrt{1 - \alpha_t}\epsilon, \sqrt{\alpha})\|^2$   
**until** converged

---

**Algorithm 2** Sampling

---

**Input:**  $N$  steps, noise schedule  $\beta_1, \dots, \beta_N$   
 $x_N \sim \mathcal{N}(0, I)$   
**for**  $t = N, \dots, 1$  **do**  
 $\epsilon \sim \mathcal{N}(0, I)$  if  $t > 1$ , else  $\epsilon = 0$   
 $x_{t-1} = \frac{1}{\sqrt{\alpha_t}} \left( x_t - \frac{1 - \alpha_t}{\sqrt{1 - \alpha_t}} \epsilon_{\theta}(x_t, \sqrt{\alpha_t}) \right) + \sigma_t \epsilon$   
**end for**  
**return**  $x_0$

---

Additionally, Ho et al. (2020) observed that the forward process can be computed for any step  $t$  such that  $q(x_t|x_0) = \mathcal{N}(x_t; \sqrt{\alpha_t}x_0, (1 - \alpha_t)I)$ , which can be viewed as a stochastic encoder. To simplify the above variational bound, Ho et al. (2020) propose training on pairs of  $(x_t, x_0)$  to learn to parameterize this process with a simple squared L2 loss. The following objective is simpler to train, resembles denoising score matching (Vincent, 2011; Song & Ermon, 2019) and was found to yield higher-quality samples:

$$L(\theta) = \mathbb{E}_{x_0, \epsilon, t} \left[ \|\epsilon - \epsilon_{\theta}(\sqrt{\alpha_t}x_0 + \sqrt{1 - \alpha_t}\epsilon, t)\|^2 \right] \quad (6)$$

where  $t$  is sampled uniformly between 1 and  $N$ ,  $\epsilon \sim \mathcal{N}(0, I)$ , and  $\epsilon_{\theta}$  is the learned diffusion model. Chen et al. (2020) found that instead of conditioning on a discrete diffusion step  $t$ , it was beneficial to sample a continuous noise level  $\sqrt{\alpha} \sim \mathbb{U}(\sqrt{\alpha_{t-1}}, \sqrt{\alpha_t})$  where  $t \sim \mathbb{U}(\{1, \dots, N\})$  and  $\alpha_0 = 1$ .

We refer readers to Algorithms 1 and 2 for the full training and sampling procedure.

## 2.2. Variational Autoencoders

Variational autoencoders (Kingma & Welling, 2014) are generative models that define  $p(y, z) = p(y|z)p(z)$  where  $z$  is a learned latent code for data point  $y$ . Additionally, the latent code is constrained such that  $z$  is distributed according to prior  $p(z)$  where the prior is usually an isotropic Gaussian. The VAE is comprised of an encoder  $q_{\gamma}(z|y)$  which models the approximate posterior  $p(z|y)$  and a decoder  $p_{\theta}(y|z)$  which models the conditional distribution of data  $y$  given latent code  $z$ .

The training objective is to maximize the log likelihood of  $p_{\theta}(x) = \int p_{\theta}(y|z)p(z)dz$ , but this marginalization is intractable, and we use the following variational bound maximized with  $q_{\gamma}(z|y)$  as the approximate posterior:

$$\mathbb{E}[\log p_{\theta}(y|z)] - \text{KL}(q_{\gamma}(z|y)||p(z)) \leq \log p(y) \quad (7)$$

The flexible implementation of variational autoencoders allows them to learn representations over a wide variety of domains. Of particular interest to us are sequential autoencoders (Bowman et al., 2016; Roberts et al., 2019) which use long short-term memory cells (Hochreiter & Schmidhuber, 1997) to model temporal context in sequential data distributions.

In practice, there is a trade-off between the quality of reconstructions and the distance between the approximate posterior  $q_{\gamma}(z|y)$  and the Gaussian prior  $p(z)$ . This makes sampling more difficult for VAEs with better reconstructions due to latent ‘‘holes’’ in the approximate posterior and is one of the primary shortcomings of these models.

## 3. Model

A diagram and description of our multi-stage diffusion model is shown in Figure 1.

### 3.1. Architecture

Our model learns to generate discrete sequences of notes (known as MIDI) by first training a VAE with parameters  $\gamma$  on the sequences and then training a diffusion model to capture the temporal relationships among the  $k$  VAE latents,  $z_k$ . Sequence VAEs such as MusicVAE are difficult to train on long sequences (Roberts et al., 2019), which we overcome by pairing the short 2-bar MusicVAE model with a diffusion model capable of modeling dependencies between 32 latents, thus modeling 64 bars in total.

**MusicVAE embeddings:** Each musical phrase is a sequence of one-hot vectors with 16 quantized steps per measure and the vocabulary contains 90 possible tokens (1 note on + 1 note off + 88 pitches). We then parameterize each 2-bar phrase using the pre-trained 2-bar melody MusicVAE (Roberts et al., 2019) and generate a sequence of continuous latent embeddings  $z_1, \dots, z_k$  to parameterize an entire sequence. As shown in Supplemental Figure 5, the MusicVAE model employs bidirectional recurrent neural networks as an encoder, and autoregressive decoding. As we use the pretrained model from the original work, full model details can be found in Roberts et al. (2019).

**Trimming latents:** After encoding each 2-measure phrase into a latent  $z$  embedding, we perform linear feature scaling such that the domain of each embedding is  $[-1, 1]$ . This ensures consistently scaled inputs starting from the isotropic Gaussian latent  $x_N$  for the diffusion model.

Additionally, during training VAEs typically learn to only utilize a fraction of their latent dimensions. As shown in Figure 2, by examining the standard deviation per dimension of the posterior  $q(z|y)$  averaged across the entire training set, we are able to identify underutilized dimensions where the average embedding standard deviation is close to the prior of 1. The VAE loss encourages the marginal posterior to match to the prior (Hoffman & Johnson; Alemi et al., 2018), but to encode information, dimensions must have smaller variance per an example.

In all experiments, we remove all dimensions except for the 42 dimensions with standard deviations below 1.0, before training the diffusion model on the input data. We find this latent trimming to be essential for training as it helps to avoid modeling unnecessary high-dimensional noise and is very similar to the distance penalty described in Engel et al. (2017a). We also tried reducing the dimensionality of embeddings with principal component analysis (PCA) but found that the lower dimensional representation captured too many of the noisy dimensions and not those with high utilization.

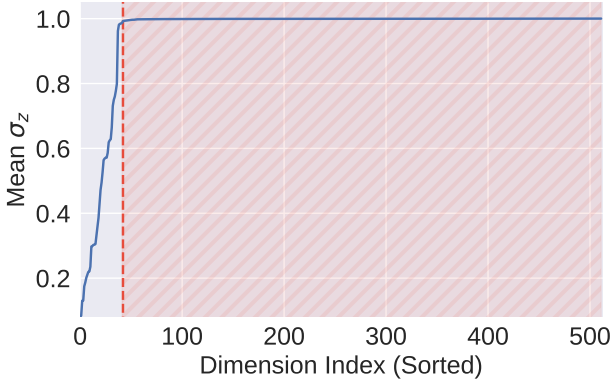


Figure 2. The standard deviation per dimension of the MusicVAE posterior  $q(z|y)$  averaged across the entire training set. The region highlighted in red contains the latent dimensions that are unused.

**Transformer diffusion model:** Our network  $\epsilon_\theta(x_t, \sqrt{\alpha}) : \mathbb{R}^{k \times 42} \times \mathbb{R} \rightarrow \mathbb{R}^{k \times 42}$  is a transformer (Vaswani et al., 2017) where  $k = 32$  is the length of each sequence of 42-dimensional preprocessed latent embeddings. The unperturbed data distribution used to train the diffusion model is  $x_0 = [z_1, \dots, z_k]$ . The network contains an initial fully-connected layer that projects the embeddings into a 128-dimensional space, followed by  $L = 6$  encoder layers each with  $H = 8$  self-attention heads and a residual fully-connected layer. All self-attention and fully-connected layers use layer normalization (Ba et al., 2016). The output of the encoder is fed to  $K = 2$  noise-conditioned residual fully-connected layers which generate the reverse process output. Each fully-connected layer contains 2048 neurons.

We use a 128-dimensional sinusoidal positional encoding similar to Vaswani et al. (2017) where  $j$  is the position index of a latent input embedding:

$$\omega = \left[ 10^{\frac{-4 \times 0}{63}} j, \dots, 10^{\frac{-4 \times 63}{63}} j \right] \quad e_j = [\sin(\omega), \cos(\omega)] \quad (8)$$

This positional encoding  $e_1, e_2, \dots, e_k$  is added to inputs  $x_t$  before being fed through the transformer encoder layers allowing the model to capture the temporal context of the continuous inputs.

**Noise schedule and conditioning:** As described in both the original diffusion model framework (Ho et al., 2020) and in Chen et al. (2020), we use an additional sinusoidal encoding to condition the diffusion model on a continuous noise level during training and sampling. This noise encoding is identical to the positional encoding described above but with the frequency of each sinusoid scaled by 5000 to account for the updated domain. We use feature-wise linear modulation (Perez et al., 2018) to generate  $\gamma$  (scale) and  $\xi$  (shift) parameters given a noise encoding and apply the transformation  $\gamma\phi + \xi$  to the output  $\phi$  of each layer normalization block in each residual layer, allowing for effective conditioning of the diffusion model. Our model uses a linear noise schedule with  $N = 1000$  steps and  $\beta_1 = 10^{-6}$  and  $\beta_N = 0.01$ .

### 3.2. Unconditional Generation

In the unconditional generation task, the goal is to produce samples that exhibit long-term structure. Because of our multi-stage approach, this works even in the scenario where the KL divergence between the marginal posterior  $q_\gamma(z)$  and the Gaussian prior is quite large because the diffusion model accurately captures the structure of the latent space therefore improving the sample quality. Additionally, we extend the underlying VAE to samples longer than what it was trained to model by using the diffusion model to predict sequences of latent embeddings and attempt to generate unconditional samples with coherent patterns across a large number of measures.

### 3.3. Infilling

One of the benefits of using a sampling process that iteratively refines noise into data samples is that the trajectory of the reverse process can be steered and arbitrarily conditioned without the need for retraining the diffusion model. In creative domains, this post-hoc conditioning is especially useful for artists without the computational resources to modify or re-train deep models for new tasks. We demonstrate the power of diffusion modeling applied to music with conditional infilling of latent embeddings using an unconditionally trained diffusion model.

The infilling procedure extends the sampling procedure de-



scribed in Algorithm 2 by incorporating information from a partially occluded sample  $s$ . At each step of sampling, we diffuse the fixed regions of  $s$  with the forward process  $q(s_t|s) = \mathcal{N}(s_t; \sqrt{\alpha_t}s, (1 - \bar{\alpha}_t)I)$  and use a mask  $m$  to add the diffused fixed regions to the updated sample  $x_{t-1}$ . The final output  $x_0$  will be a version of  $s$  with the occluded regions inpainted by the reverse process.

We refer readers to Algorithm 3 for the modified sampling procedure that allows for post-hoc conditional infilling.

## 4. Methods

### 4.1. Data

We use the Lakh MIDI Dataset (LMD) (Raffel, 2016) for all experiments. The dataset contains over 170,000 MIDI files with 99% of those files used for training and the remaining used for validation. We extracted 988,893 64-bar monophonic sequences for training and 11,295 for validation from the provided MIDI files. Each sequence was encoded into 32 continuous latent embeddings using MusicVAE. We set the softmax temperature for MusicVAE to 0.001 for decoding generated embeddings in all experiments. A diagram of the MusicVAE architecture used is shown in the supplementary material.

### 4.2. Autoregressive Baseline

We compare our model to an autoregressive transformer with a mixture density output layer (Bishop, 1994) and train on the same dataset as the diffusion model. To ensure a fair comparison, we use the same architecture as our diffusion model with  $L = 6$ ,  $H = 8$ , and  $K = 2$  with 2048 neurons for each fully-connected layer. The mixture density layer uses 100 output mixtures to ensure sufficient mode coverage. In total, our baseline model has 38M trainable parameters. While the model is the same as the diffusion model (25.58M trainable parameters) up until the output layer, the autoregressive model has more parameters due to the much larger output layer. We refer to this model as TransformerMDN.

### 4.3. Training

All models were trained using Adam (Kingma & Ba, 2014) with default parameters. We trained our diffusion model for 500K gradient updates on a single NVIDIA Tesla V100 GPU for 6.5 hours using a learning rate of  $10^{-3}$  annealed with a decay rate of 0.98 every 4000 steps and batch size 64. Unlike the diffusion model, which is non-autoregressive, we train TransformerMDN with teacher forcing. We use a batch size of 128, learning rate  $3 \times 10^{-4}$ , and train for 250K gradient updates on a single NVIDIA Tesla V100 GPU for 6.5 hours.

We used the open-source implementation of MusicVAE

---

### Algorithm 3 Infilling

---

**Input:** mask  $m$ , sample  $s$ ,  $N$  steps,  $\beta_1, \dots, \beta_N$   
 $x_N \sim \mathcal{N}(0, I)$   
**for**  $t = N, \dots, 1$  **do**  
 $\epsilon_1, \epsilon_2 \sim \mathcal{N}(0, I)$  if  $t > 1$ , else  $\epsilon_1 = \epsilon_2 = 0$   
 $y = \sqrt{\alpha_t}s + \sqrt{1 - \bar{\alpha}_t}\epsilon_1$  if  $t > 1$ , else  $s$   
 $x_{t-1} = \frac{1}{\sqrt{\alpha_t}} \left( x_t - \frac{1 - \alpha_t}{\sqrt{1 - \bar{\alpha}_t}} \epsilon_\theta(x_t, \sqrt{\bar{\alpha}_t}) \right) + \sigma_t \epsilon_2$   
 $x_{t-1} = x_{t-1} \odot (1 - m) + y \odot m$   
**end for**  
**return**  $x_0$

---

written in TensorFlow (Abadi et al., 2016) and the publicly available 2-bar melody checkpoints trained on the Lakh MIDI Dataset. We trained our diffusion and baseline models<sup>1</sup> with JAX (Bradbury et al., 2018) and Flax (Heek et al., 2020).

### 4.4. Framewise Self-similarity Metric

Inspired by the statistical similarity evaluation described in Choi et al. (2020), we evaluate our models with a modified framewise Overlapping Area (OA) metric. The goal of this metric is to capture local self-similarity patterns across a generated sequence and yield a statistic that effectively represents the qualitative output of our models.

We use a sliding 4-measure window with 2-measure hop size to capture local pitch and duration statistics across the piece. Within each 4-measure frame, we compute the mean and variance of both pitch, which captures melodic similarity, and duration, which captures rhythmic similarity. These statistics specify a Gaussian PDF for pitch and duration for each frame ( $p_P(k), p_D(k)$ ). We compute the Overlapping Area (OA) (Choi et al., 2020) of adjacent frames ( $k, k + 1$ ) where each frame’s statistics are modeled as  $\mathcal{N}(\mu_1, \sigma_1^2)$  and  $\mathcal{N}(\mu_2, \sigma_2^2)$ , respectively:

$$OA(k, k + 1) = 1 - \operatorname{erf} \left( \frac{c - \mu_1}{\sqrt{2}\sigma_1^2} \right) + \operatorname{erf} \left( \frac{c - \mu_2}{\sqrt{2}\sigma_2^2} \right) \quad (9)$$

for both pitch ( $OA_P$ ) and duration ( $OA_D$ ), where  $\operatorname{erf}$  is the Gauss error function and  $c$  is the point of intersection between Gaussian PDFs with  $\mu_1 < \mu_2$ . For a set of MIDI samples, we infer the *Consistency* and *Variance* from the mean ( $\mu_{OA}$ ) and variance ( $\sigma_{OA}^2$ ) respectively of OA aggregated over all adjacent frames. We then use these aggregate values to compute the normalized relative similarity of pitch and duration consistency and variance to the training set

---

<sup>1</sup>Our implementation is available at <https://github.com/magenta/symbolic-music-diffusion>

Table 1. Framework self-similarity of consistency and variance (as defined in Equation 10) for note pitch and duration. For both unconditional sampling and infilling tasks, the diffusion model produces samples most similar to the real data. For diffusion samples, we use  $N = 1000$  sampling steps with  $\beta_1 = 10^{-6}$  and  $\beta_N = 0.01$ . For the TransformerMDN baseline we sample with a temperature of 1.0, meaning we sampled directly from the logits of mixture density layer. Absolute values of overlap area can be found in Supplemental Table 2.

SETTING	UNCONDITIONAL				INFILLING			
QUANTITY	PITCH		DURATION		PITCH		DURATION	
CONSISTENCY/VARIANCE	C	VAR	C	VAR	C	VAR	C	VAR
TRAIN	1.00	1.00	1.00	1.00	1.00	1.00	1.00	1.00
TEST	1.00	0.96	1.00	0.91	1.00	0.96	1.00	0.91
DIFFUSION	<b>0.99</b>	<b>0.90</b>	<b>0.96</b>	<b>0.92</b>	<b>0.97</b>	<b>0.87</b>	<b>0.97</b>	<b>0.80</b>
AUTOREGRESSION	0.93	0.68	0.93	0.76	-	-	-	-
INTERPOLATION	0.85	0.23	0.91	0.34	0.94	0.78	0.96	<b>0.80</b>
$\mathcal{N}(0, I)$ PRIOR	0.84	0.19	0.90	0.67	0.89	0.19	0.94	0.54

(GT):

$$\begin{aligned}
 \text{Consistency} &= \max(0, 1 - \frac{|\mu_{OA} - \mu_{GT}|}{\mu_{GT}}) \\
 \text{Variance} &= \max(0, 1 - \frac{|\sigma_{OA}^2 - \sigma_{GT}^2|}{\sigma_{GT}^2})
 \end{aligned} \quad (10)$$

We clip *Consistency* and *Variance* such that samples with  $\mu_{OA}$  or  $\sigma_{OA}^2$  with greater than 100% percent error from the ground truth are considered to have zero relative similarity to the training set.

#### 4.5. Latent Space Evaluation

We evaluate the similarity of latent embeddings generated by each of our models using the Fréchet distance (FD) (Heusel et al., 2018) and Maximum Mean Discrepancy (MMD) (Gretton et al., 2012) with a polynomial kernel. These metrics measure the distance between the models’ continuous output distributions and the original data distribution in latent space. It is important to note that this metric does not measure long-term temporal consistency or quality of produced sequences and only measures the quality of the intermediate continuous representation before the final sequence is generated using the MusicVAE decoder.

## 5. Results

### 5.1. Unconditional Generation

To evaluate unconditional sample quality, we compare batches of 1000 samples (32 latents each) generated by our proposed diffusion model with random draws from the training and test sets. We compare against a set of baseline generators including TransformerMDN, the independent  $\mathcal{N}(0, I)$  MusicVAE prior, and spherical interpolation (White, 2016) between two MusicVAE embeddings at the start and finish of an example from the test set.

As seen in Table 1, the diffusion model quantitatively produces samples most similar to the training data according to the relative framework overlapping area metrics for note pitch and duration. The diffusion model outperforms TransformerMDN, which is challenged by modelling the relatively high-dimensional continuous latents autoregressively, even with a mixture of Gaussians output. The autoregressive models are also trained with teacher forcing that results in exposure bias, leading to divergence from the data distribution during sampling. This is reflected in the lower pitch and duration consistency and higher variance in the absolute overlapping area numbers seen in Supplemental Table 2. Additionally, the diffusion model is able to capture the joint dependencies of the sequences better because it learns to model all latents simultaneously as opposed to autoregressively. Note that the Gaussian prior also suffers from low consistency and high variance, due to lack of temporal dependencies, while the interpolated samples conversely suffer from low variance and too much consistency due to high repetition.

Supplemental Table 3, presents latent space evaluations of our generated samples. The TransformerMDN outperformed all other models, likely due to the Gaussian mixture prior on its output layer whereas the diffusion model must learn the output distribution from scratch. Furthermore, the latent space metrics are limited by assumptions made about the distribution of the latent manifold and it also possible that these metrics are not able to fully capture the detail of the entire space, further highlighting the necessity of our quantitative framework self-similarity metrics and qualitative evaluations.

Figure 4 helps us to further understand the iterative refinement process by showing the improvement in sample quality as a function of iterative refinement time for both latent space and framework self-similarity metrics. Interestingly, latent metrics improve steadily, while consistency similarity

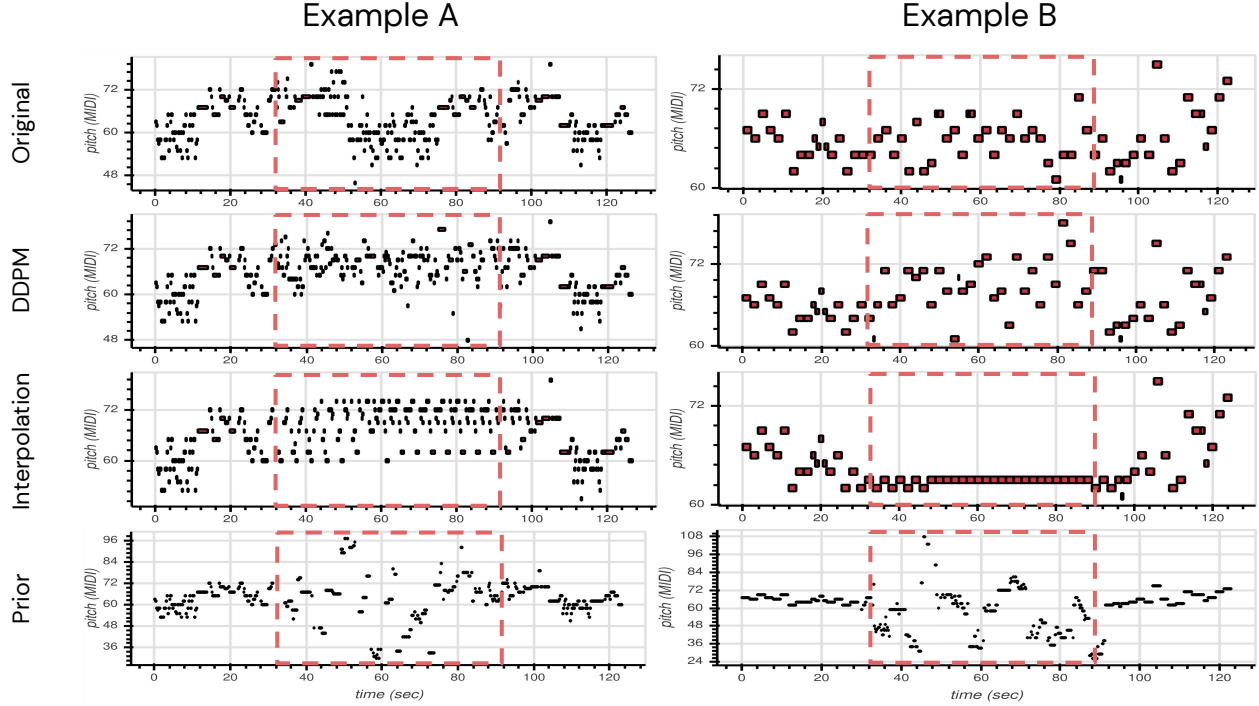


Figure 3. Example piano rolls of infilling experiments. For each example (A, B) the first and last 256 melody tokens are held constant, and the interior 512 tokens are filled in by the model (dashed red box). Even qualitatively, it is visually apparent that the diffusion model (second row) produces notes with a consistency and variance similar to the original data (first row), while the latent interpolation (third row) is too repetitive, and sampling independently from the prior (last row) produces outputs with too much variety and lack of local coherence.

starts fairly high, and variance similarity only emerges at the end of refinement. We refer the reader to the supplementary material for extended visual and audio samples of the generated sequences from each model<sup>2</sup>.

## 5.2. Infilling

To probe the diffusion model’s ability to perform post-hoc conditional generation, we remove the middle 32 measures (16 embeddings) and generate new embeddings following Algorithm 3 by conditioning on the first and last 8 embeddings. As in the unconditional setting, we compare to interpolation and independent samples from the prior.

Figure 3, visualizes the task by plotting the resulting note sequences for two different examples. Even qualitatively, it is visually apparent that the diffusion model produces notes with a consistency and variance similar to the original data. Latent interpolation is very consistent but unrealistically repetitive, and sampling independently from the prior produces a sequence with extremely large variance that is inconsistent in both pitch and duration.

<sup>2</sup><https://goo.gl/magenta/symbolic-music-diffusion-examples>

The quantitative evaluations in Table 1 back up these observations. Similar to the unconditional generation task, the diffusion model outperforms the baselines in both consistency and variance similarity. We do not include the autoregressive baseline because it is not able to condition on the final 8 embeddings.

## 6. Related Work

**Multi-stage learning:** Several models have achieved long-term structure by first modeling some intermediate representation and then using that to guide the final generative process. Wave2Midi2Wave (Hawthorne et al., 2019) uses a transformer to generate MIDI-like symbolic data and then a Wavenet (Oord et al., 2016) to synthesize that symbolic data into audio. VQ-VAE-2 (Razavi et al., 2019) learns a hierarchy of discrete image embeddings that are decoded using an autoregressive model. Jukebox (Dhariwal et al., 2020) and DALL-E (Ramesh et al., 2021) use similar approaches for text-conditioned generative music audio and image models.

A related approach has been to refine the output of a VAE (Kingma & Welling, 2014) with an energy-based model (Xiao et al., 2020) or use an additional model to con-

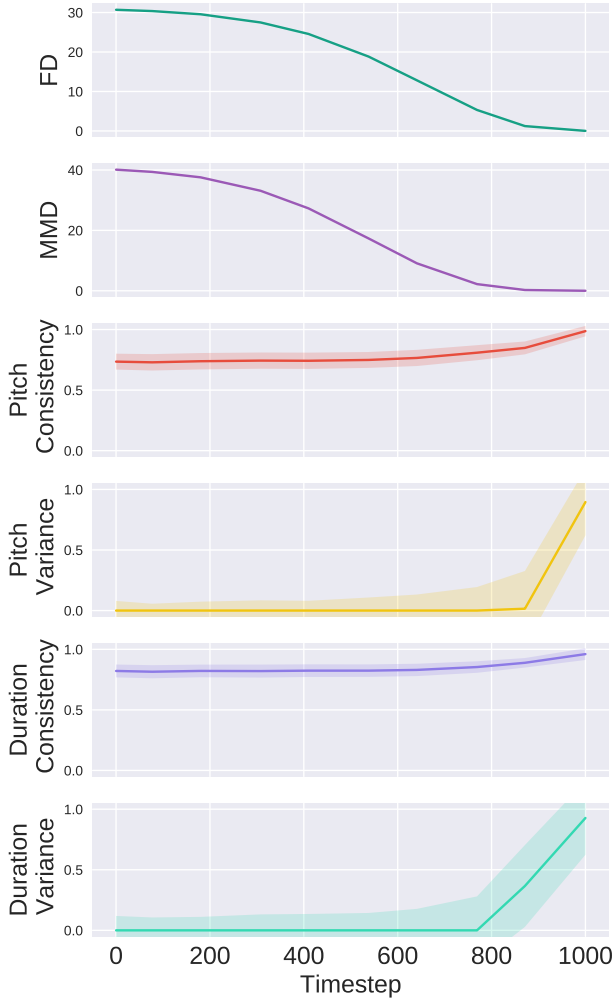


Figure 4. Sample quality improvement during iterative refinement. Latent space and framewise metrics evaluated at different stages of unconditional sampling. The metrics improve as the iterative refinement process progresses and we plot the means and standard deviations for a batch of 1000 samples.

strain the VAE’s prior before sampling (Engel et al., 2017a; Aneja et al., 2020). In the music domain, there has also been work investigating the extension of a single-measure VAE to multiple measures by using an autoregressive LSTM with a mixture density output layer (Jhamtani & Berg-Kirkpatrick, 2019).

**Iterative refinement:** In the music domain, Huang et al. (2017) use an orderless NADE with blocked Gibbs sampling to iteratively rewrite musical harmonies based on surrounding context. Lattner et al. (2016) use a gradient-based sampler combined with a restricted Boltzmann machine to generate polyphonic piano music. Similarly, Zhang & Sirohi (2020) investigated the use of a noise-conditional score network (Song & Ermon, 2019) to generate Bach chorales with

annealed Langevin dynamics. A key distinction between our method and prior work is the use of a variational autoencoder to parameterize the discrete space of musical notes into a continuous manifold for improved training and sampling with a diffusion model while previous methods have performed iterative refinement in the discrete space directly.

**Conditional sampling from unconditional models:** We build on top of the breadth of material that explores conditional sampling from unconditionally trained models by using an additional model to steer generation in the latent space of an unconditionally trained generative model (Nguyen et al., 2017; Jaques et al., 2018; Jahanian et al., 2019; Dathathri et al., 2019). An exception to this is the recent work in energy-based and score-based generative modeling where the composition of energy functions and flexibility of Langevin dynamics has allowed for conditional sampling in the data space directly (Du & Mordatch, 2020; Song et al., 2020). However, these techniques have been limited to continuous data spaces due to the gradient-based sampling mechanisms that they use.

Most similar to our work is Nguyen et al. (2017); Engel et al. (2017a); Dinculescu et al. (2019) which train an additional model on top of a pre-trained variational autoencoder to steer generation in the latent space of that autoencoder. Our approach builds on top of this by not only improving sampling and generation of the underlying autoencoder but also extending generation to sequences much longer than those used to train the VAE. We also use a diffusion model to refine generation and provide conditional infilling while the works mentioned primarily used conditional GANs and VAEs to extend the underlying autoencoder for a single latent embedding as opposed to a sequence of latent embeddings.

## 7. Conclusion

We have proposed and demonstrated a multi-stage generative model comprised of a low-level variational autoencoder with continuous latents modeled by a higher-level diffusion model. This model enables using diffusion models on discrete data, and as priors for modeling long-term structure in multi-stage systems. We demonstrate that this model is useful for symbolic music generation, both in unconditional generation and conditional infilling. Future work can include extending this approach to other discrete data such as text, and exploring a greater array of approaches for post-hoc conditioning in creative applications.

## Acknowledgements

The authors wish to thank Anna Huang, Carrie Cai, Sander Dieleman, Doug Eck and the rest of the Magenta team for helpful discussions, inspiration, and encouragement.



## References

- Abadi, M., Barham, P., Chen, J., Chen, Z., Davis, A., Dean, J., Devin, M., Ghemawat, S., Irving, G., Isard, M., et al. Tensorflow: A system for large-scale machine learning. In *12th {USENIX} symposium on operating systems design and implementation ({OSDI} 16)*, pp. 265–283, 2016.
- Alemi, A., Poole, B., Fischer, I., Dillon, J., Saourous, R. A., and Murphy, K. Fixing a broken elbo. In *International Conference on Machine Learning*, pp. 159–168. PMLR, 2018.
- Aneja, J., Schwing, A., Kautz, J., and Vahdat, A. Ncp-vae: Variational autoencoders with noise contrastive priors, 2020.
- Ba, J. L., Kiros, J. R., and Hinton, G. E. Layer normalization. *arXiv preprint arXiv:1607.06450*, 2016.
- Bishop, C. M. Mixture density networks. 1994.
- Bowman, S. R., Vilnis, L., Vinyals, O., Dai, A. M., Jozefowicz, R., and Bengio, S. Generating sentences from a continuous space, 2016.
- Bradbury, J., Frostig, R., Hawkins, P., Johnson, M. J., Leary, C., Maclaurin, D., Necula, G., Paszke, A., VanderPlas, J., Wanderman-Milne, S., and Zhang, Q. JAX: composable transformations of Python+NumPy programs, 2018. URL <http://github.com/google/jax>.
- Chen, N., Zhang, Y., Zen, H., Weiss, R. J., Norouzi, M., and Chan, W. Wavegrad: Estimating gradients for waveform generation, 2020.
- Choi, K., Hawthorne, C., Simon, I., Dinculescu, M., and Engel, J. Encoding musical style with transformer autoencoders. In *International Conference on Machine Learning*, pp. 1899–1908. PMLR, 2020.
- Dathathri, S., Madotto, A., Lan, J., Hung, J., Frank, E., Molino, P., Yosinski, J., and Liu, R. Plug and play language models: A simple approach to controlled text generation. *arXiv preprint arXiv:1912.02164*, 2019.
- Dhariwal, P., Jun, H., Payne, C., Kim, J. W., Radford, A., and Sutskever, I. Jukebox: A generative model for music. *arXiv preprint arXiv:2005.00341*, 2020.
- Dinculescu, M., Engel, J., and Roberts, A. (eds.). *MidiMe: Personalizing a MusicVAE model with user data*, 2019.
- Donahue, C., Simon, I., and Dieleman, S. Piano genie. *Proceedings of the 24th International Conference on Intelligent User Interfaces*, Mar 2019. doi: 10.1145/3301275.3302288. URL <http://dx.doi.org/10.1145/3301275.3302288>.
- Du, Y. and Mordatch, I. Implicit generation and generalization in energy-based models, 2020.
- Engel, J., Hoffman, M., and Roberts, A. Latent constraints: Learning to generate conditionally from unconditional generative models, 2017a.
- Engel, J., Resnick, C., Roberts, A., Dieleman, S., Eck, D., Simonyan, K., and Norouzi, M. Neural audio synthesis of musical notes with wavenet autoencoders. 2017b. URL <https://arxiv.org/abs/1704.01279>.
- Engel, J., Agrawal, K. K., Chen, S., Gulrajani, I., Donahue, C., and Roberts, A. GANSynth: Adversarial neural audio synthesis. In *International Conference on Learning Representations*, 2019. URL <https://openreview.net/forum?id=H1xQVn09FX>.
- Engel, J., Hantrakul, L. H., Gu, C., and Roberts, A. Ddsp: Differentiable digital signal processing. In *International Conference on Learning Representations*, 2020. URL <https://openreview.net/forum?id=B1x1ma4tDr>.
- Goodfellow, I. J., Pouget-Abadie, J., Mirza, M., Xu, B., Warde-Farley, D., Ozair, S., Courville, A., and Bengio, Y. Generative adversarial networks. *arXiv preprint arXiv:1406.2661*, 2014.
- Gretton, A., Borgwardt, K. M., Rasch, M. J., Schölkopf, B., and Smola, A. A kernel two-sample test. *Journal of Machine Learning Research*, 13(25):723–773, 2012. URL <http://jmlr.org/papers/v13/gretton12a.html>.
- Hawthorne, C., Stasyuk, A., Roberts, A., Simon, I., Huang, C.-Z. A., Dieleman, S., Elsen, E., Engel, J., and Eck, D. Enabling factorized piano music modeling and generation with the MAESTRO dataset. In *International Conference on Learning Representations*, 2019. URL <https://openreview.net/forum?id=r11YRjC9F7>.
- Heek, J., Levskaya, A., Oliver, A., Ritter, M., Rondepierre, B., Steiner, A., and van Zee, M. Flax: A neural network library and ecosystem for JAX, 2020. URL <http://github.com/google/flax>.
- Heusel, M., Ramsauer, H., Unterthiner, T., Nessler, B., and Hochreiter, S. Gans trained by a two time-scale update rule converge to a local nash equilibrium, 2018.
- Ho, J., Jain, A., and Abbeel, P. Denoising diffusion probabilistic models. *arXiv preprint arxiv:2006.11239*, 2020.
- Hochreiter, S. and Schmidhuber, J. Long short-term memory. *Neural computation*, 9(8):1735–1780, 1997.

- Hoffman, M. D. and Johnson, M. J. Elbo surgery: yet another way to carve up the variational evidence lower bound.
- Huang, C.-Z. A., Cooijmans, T., Roberts, A., Courville, A., and Eck, D. Counterpoint by convolution. In *Proceedings of ISMIR 2017*, 2017. URL [https://ismir2017.smcnus.org/wp-content/uploads/2017/10/187\\_Paper.pdf](https://ismir2017.smcnus.org/wp-content/uploads/2017/10/187_Paper.pdf).
- Huang, C.-Z. A., Vaswani, A., Uszkoreit, J., Simon, I., Hawthorne, C., Shazeer, N., Dai, A. M., Hoffman, M. D., Dinculescu, M., and Eck, D. Music transformer: Generating music with long-term structure. In *International Conference on Learning Representations*, 2018.
- Huang, Y.-S. and Yang, Y.-H. Pop music transformer: Generating music with rhythm and harmony. *arXiv preprint arXiv:2002.00212*, 2020.
- Jahani, A., Chai, L., and Isola, P. On the “steerability” of generative adversarial networks. *arXiv preprint arXiv:1907.07171*, 2019.
- Jacques, N., Engel, J., Ha, D., Bertsch, F., Picard, R., and Eck, D. Learning via social awareness: improving sketch representations with facial feedback. In *International Conference on Learning Representations*, 2018. URL <https://arxiv.org/abs/1802.04877>. Workshop Track.
- Jhamtani, H. and Berg-Kirkpatrick, T. Modeling self-repetition in music generation using generative adversarial networks. 2019.
- Kingma, D. P. and Ba, J. Adam: A method for stochastic optimization. *arXiv preprint arXiv:1412.6980*, 2014.
- Kingma, D. P. and Welling, M. Auto-encoding variational bayes. In *Second International Conference on Learning Representations*, 2014.
- Kong, Z., Ping, W., Huang, J., Zhao, K., and Catanzaro, B. Diffwave: A versatile diffusion model for audio synthesis. *arXiv preprint arXiv:2009.09761*, 2020.
- Lattner, S., Grachten, M., and Widmer, G. Imposing higher-level structure in polyphonic music generation using convolutional restricted boltzmann machines and constraints. *arXiv preprint arXiv:1612.04742*, 2016.
- Nguyen, A., Clune, J., Bengio, Y., Dosovitskiy, A., and Yosinski, J. Plug & play generative networks: Conditional iterative generation of images in latent space. In *Proceedings of the IEEE Conference on Computer Vision and Pattern Recognition*, pp. 4467–4477, 2017.
- Oord, A. v. d., Dieleman, S., Zen, H., Simonyan, K., Vinyals, O., Graves, A., Kalchbrenner, N., Senior, A., and Kavukcuoglu, K. Wavenet: A generative model for raw audio. *arXiv preprint arXiv:1609.03499*, 2016.
- Payne, C. Musenet, 2019. URL [openai.com/blog/musenet](https://openai.com/blog/musenet).
- Perez, E., Strub, F., De Vries, H., Dumoulin, V., and Courville, A. Film: Visual reasoning with a general conditioning layer. In *Proceedings of the AAAI Conference on Artificial Intelligence*, volume 32, 2018.
- Raffel, C. *Learning-based methods for comparing sequences, with applications to audio-to-midi alignment and matching*. PhD thesis, Columbia University, 2016.
- Ramesh, A., Pavlov, M., Goh, G., Gray, S., Chen, M., Child, R., Misra, V., Mishkin, P., Krueger, G., Agarwal, S., and Sutskever, I. Dall-e: Creating images from text. *OpenAI blog*, 2021. URL <https://openai.com/blog/dall-e>.
- Razavi, A., van den Oord, A., and Vinyals, O. Generating diverse high-fidelity images with vq-vae-2, 2019.
- Roberts, A., Engel, J., Raffel, C., Hawthorne, C., and Eck, D. A hierarchical latent vector model for learning long-term structure in music, 2019.
- Simon, I., Roberts, A., Raffel, C., Engel, J., Hawthorne, C., and Eck, D. Learning a latent space of multitrack measures, 2018.
- Sohl-Dickstein, J., Weiss, E., Maheswaranathan, N., and Ganguli, S. Deep unsupervised learning using nonequilibrium thermodynamics. In Bach, F. and Blei, D. (eds.), *Proceedings of the 32nd International Conference on Machine Learning*, volume 37 of *Proceedings of Machine Learning Research*, pp. 2256–2265, Lille, France, 07–09 Jul 2015. PMLR. URL <http://proceedings.mlr.press/v37/sohl-dickstein15.html>.
- Song, Y. and Ermon, S. Generative modeling by estimating gradients of the data distribution. *arXiv preprint arXiv:1907.05600*, 2019.
- Song, Y. and Ermon, S. Improved techniques for training score-based generative models. *arXiv preprint arXiv:2006.09011*, 2020.
- Song, Y., Sohl-Dickstein, J., Kingma, D. P., Kumar, A., Ermon, S., and Poole, B. Score-based generative modeling through stochastic differential equations. *arXiv preprint arXiv:2011.13456*, 2020.
- Vaswani, A., Shazeer, N., Parmar, N., Uszkoreit, J., Jones, L., Gomez, A. N., Kaiser, L., and Polosukhin, I. Attention is all you need. *arXiv preprint arXiv:1706.03762*, 2017.

- Vincent, P. A connection between score matching and denoising autoencoders. *Neural computation*, 23(7):1661–1674, 2011.
- Wang, Z., Zhang, Y., Zhang, Y., Jiang, J., Yang, R., Zhao, J., and Xia, G. Pianotree vae: Structured representation learning for polyphonic music. *arXiv preprint arXiv:2008.07118*, 2020.
- White, T. Sampling generative networks. *arXiv preprint arXiv:1609.04468*, 2016.
- Xiao, Z., Kreis, K., Kautz, J., and Vahdat, A. Vaebm: A symbiosis between variational autoencoders and energy-based models, 2020.
- Zhang, E. and Sirohi, R. Generative modeling of bach chorales by gradient estimation, 2020. URL [https://www.ekzhang.com/assets/pdf/Generative\\_Music\\_Modeling.pdf](https://www.ekzhang.com/assets/pdf/Generative_Music_Modeling.pdf).

## A. MusicVAE Architecture

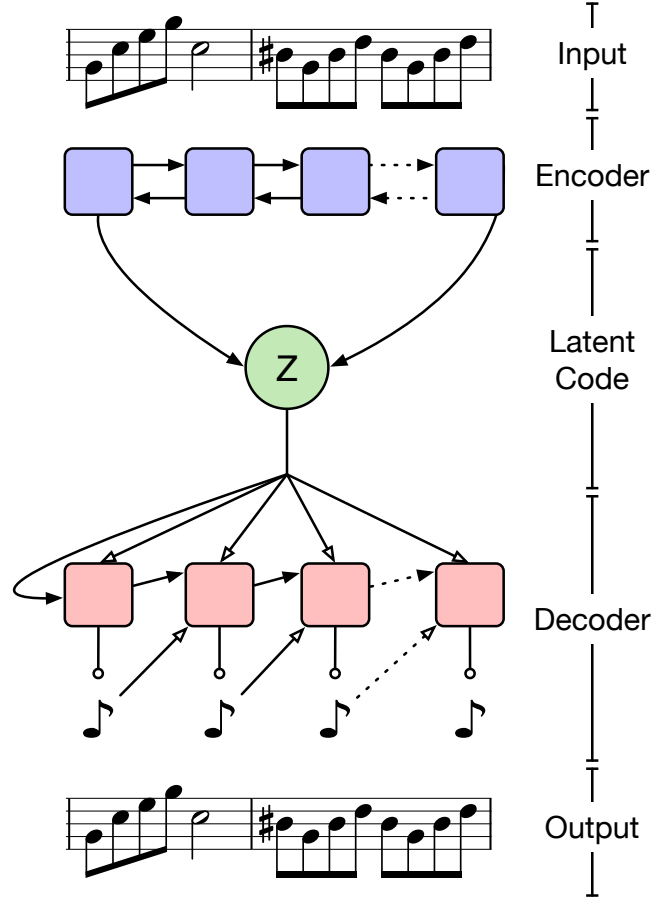


Figure 5. 2-bar melody MusicVAE architecture. The encoder is a bi-direction LSTM and the decoder is an autoregressive LSTM.

## B. Tables

In Tables 2 and 3, we present the unnormalized framewise self-similarity results as well as the latent space evaluation of each model.

## C. Additional Samples

In Figure 6 we provide piano rolls of sequences drawn from the test set and in Figures 7, 8, 9, and 10 we present additional samples unconditionally generated by our diffusion model, TransformerMDN, spherical interpolation, and through independent sampling from the MusicVAE prior, respectively. Additional piano roll visualizations from infilling experiments are provided in Figure 11.

For extended visual and audio samples of the generated sequences from each model, we refer the reader to the online supplement available at <https://goo.gl/magenta/symbolic-music-diffusion-examples>.

Table 2. Unnormalized framewise self-similarity (overlapping area) evaluation of unconditional and conditional samples. Evaluations of same samples as in Table 1. Note the interpolations have unrealistically high mean overlap and low variance, while the Gaussian prior and TransformerMDN samples suffer from unrealistically lower mean overlap and higher variance.

SETTING	UNCONDITIONAL				INFILLING			
QUANTITY	PITCH		DURATION		PITCH		DURATION	
OA	$\mu$	$\sigma^2$	$\mu$	$\sigma^2$	$\mu$	$\sigma^2$	$\mu$	$\sigma^2$
TRAIN	0.82	0.018	0.88	0.012	0.82	0.018	0.88	0.012
TEST	0.82	0.018	0.88	0.011	0.82	0.018	0.88	0.011
DIFFUSION	<b>0.81</b>	<b>0.017</b>	<b>0.85</b>	<b>0.013</b>	<b>0.80</b>	<b>0.021</b>	<b>0.86</b>	<b>0.015</b>
AUTOREGRESSION	0.76	0.024	0.82	0.015	-	-	-	-
INTERPOLATION	0.94	0.004	0.96	0.004	0.87	0.014	0.91	<b>0.009</b>
$\mathcal{N}(0, I)$ PRIOR	0.69	0.033	0.79	0.016	0.73	0.033	0.82	0.018

Table 3. Latent space evaluation of infilling and unconditional and conditional samples. As described in Section 4.5, the TransformerMDN performs better in latent space similarity, even while producing less realistic samples (as seen in Tables 1 and Supplemental 2).

SETTING	UNCONDITIONAL		INFILLING	
	$FD \times 10^{-2}$	$MMD \times 10^{-2}$	$FD \times 10^{-2}$	$MMD \times 10^{-2}$
TRAIN	0.00	0.00	0.00	0.00
TEST	1.24	0.12	1.24	0.12
DIFFUSION	1.66	0.18	1.53	0.16
AUTOREGRESSION	<b>1.26</b>	<b>0.12</b>	-	-
INTERPOLATION	3.22	0.43	1.97	0.23
$\mathcal{N}(0, I)$ PRIOR	2.44	0.29	<b>1.17</b>	<b>0.12</b>



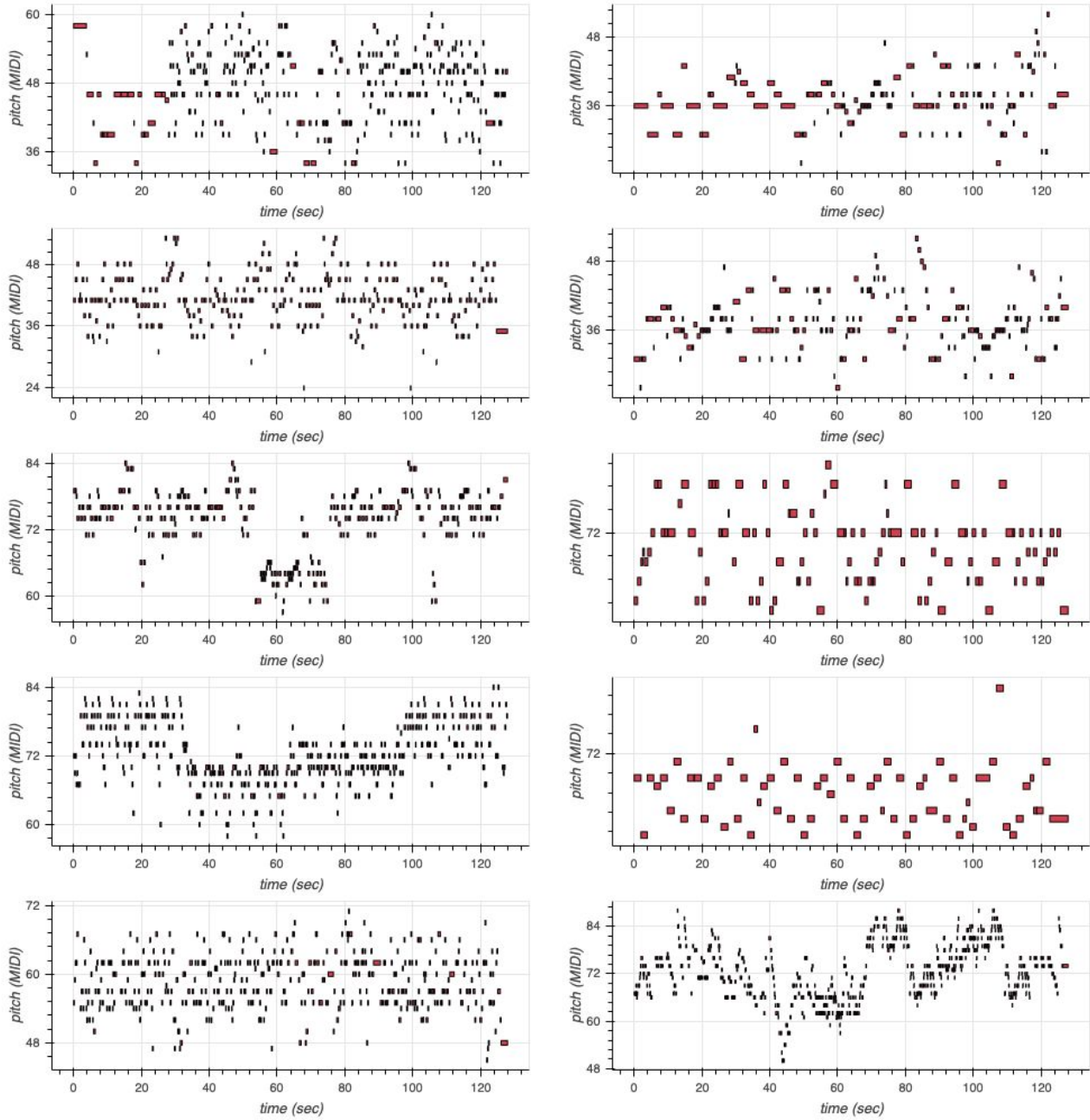


Figure 6. Additional piano rolls from the test set.

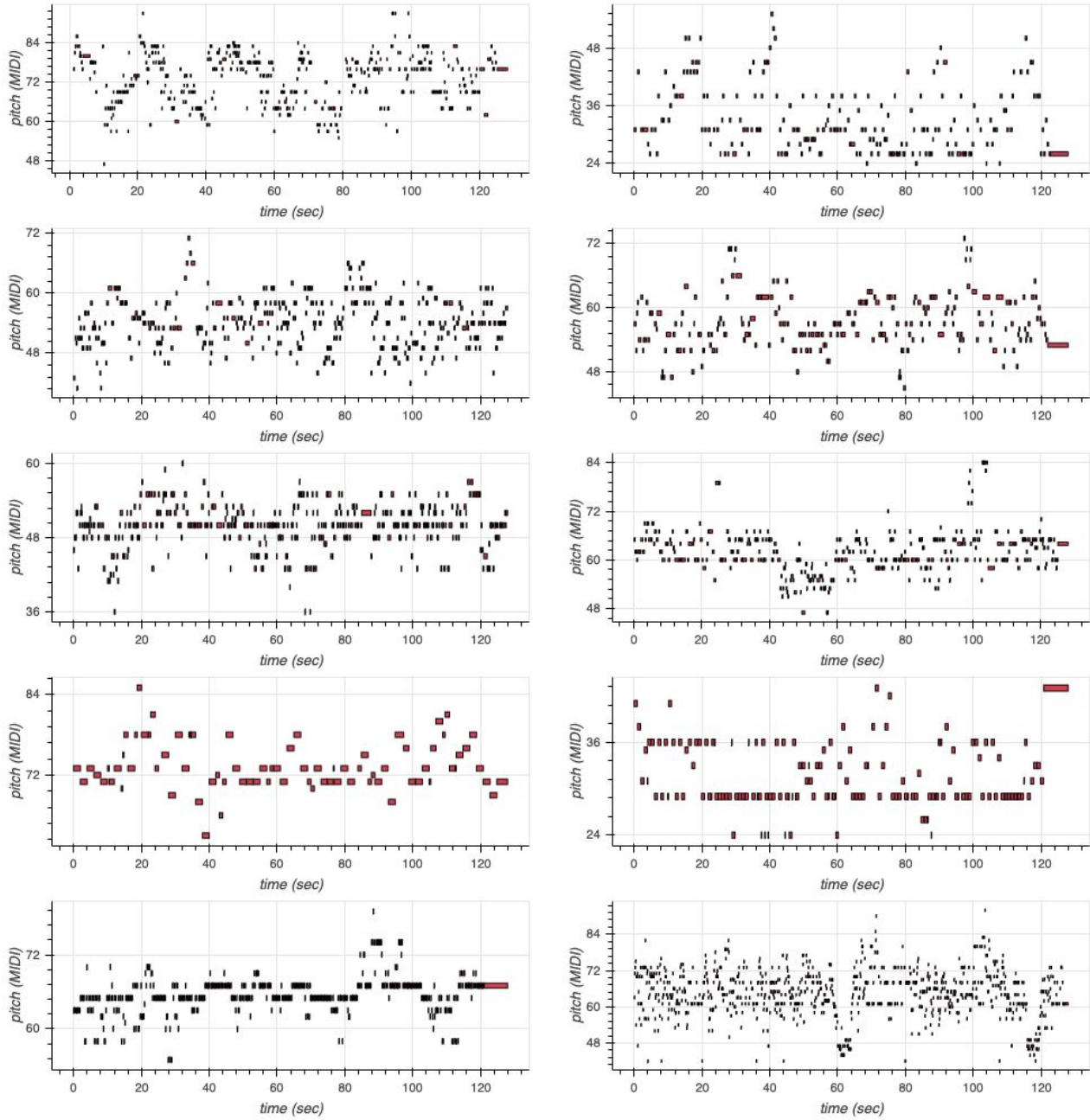


Figure 7. Additional piano rolls generated unconditionally by our diffusion model.

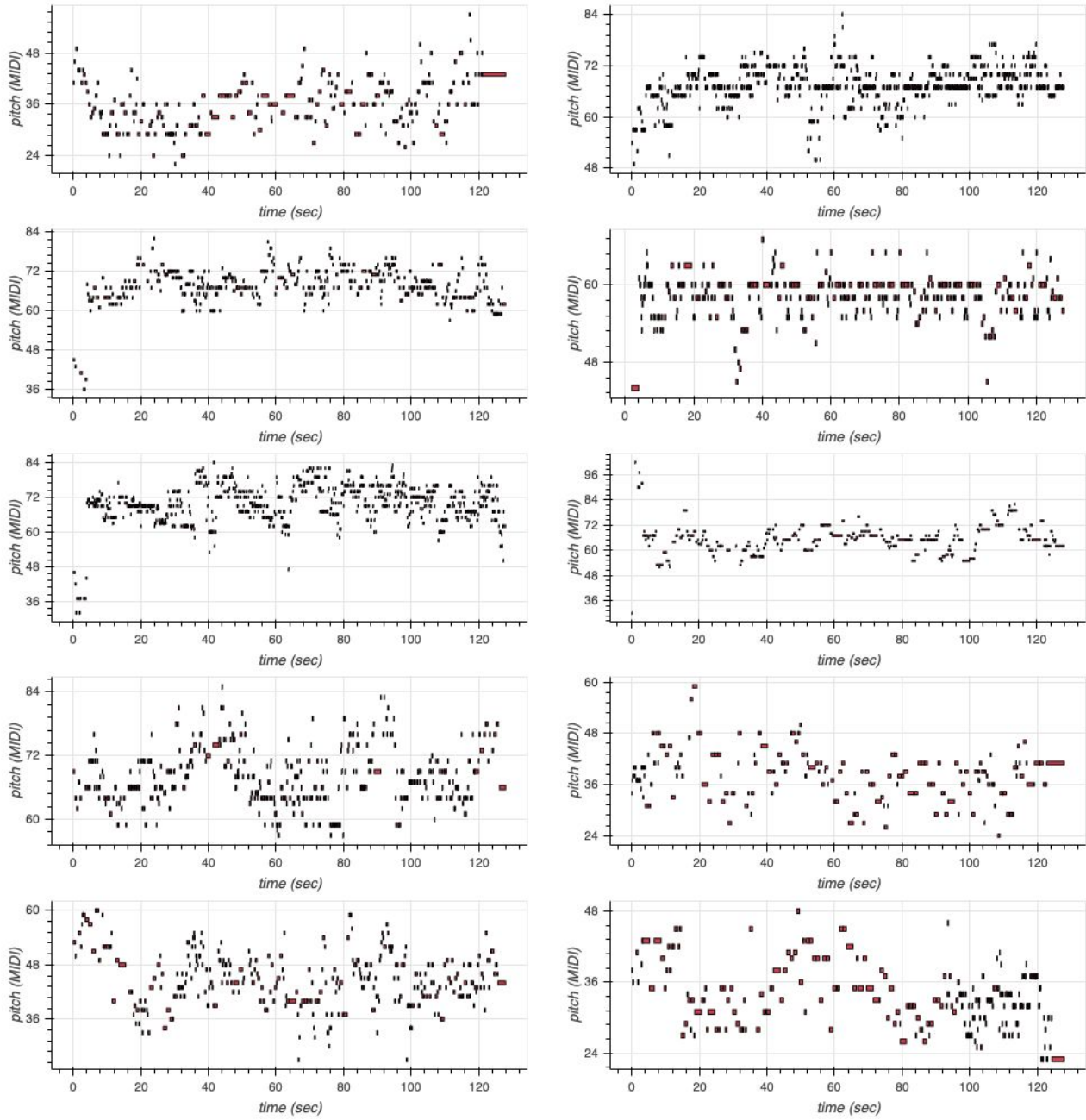


Figure 8. Additional piano rolls generated unconditionally by TransformerMDN.

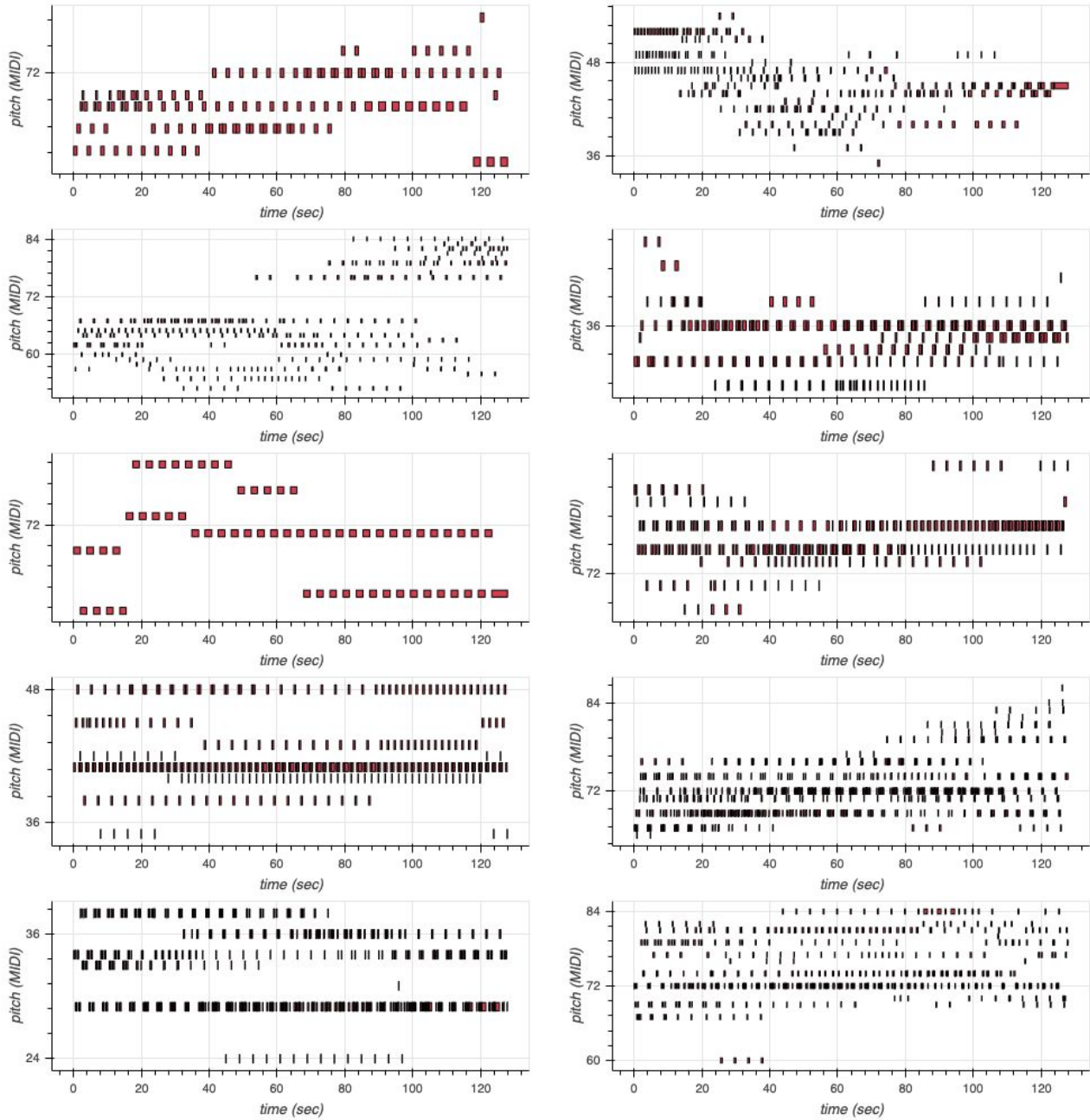


Figure 9. Additional piano rolls generated by performing spherical interpolation (White, 2016) between the first and last latent embeddings of sequences drawn from the test set.



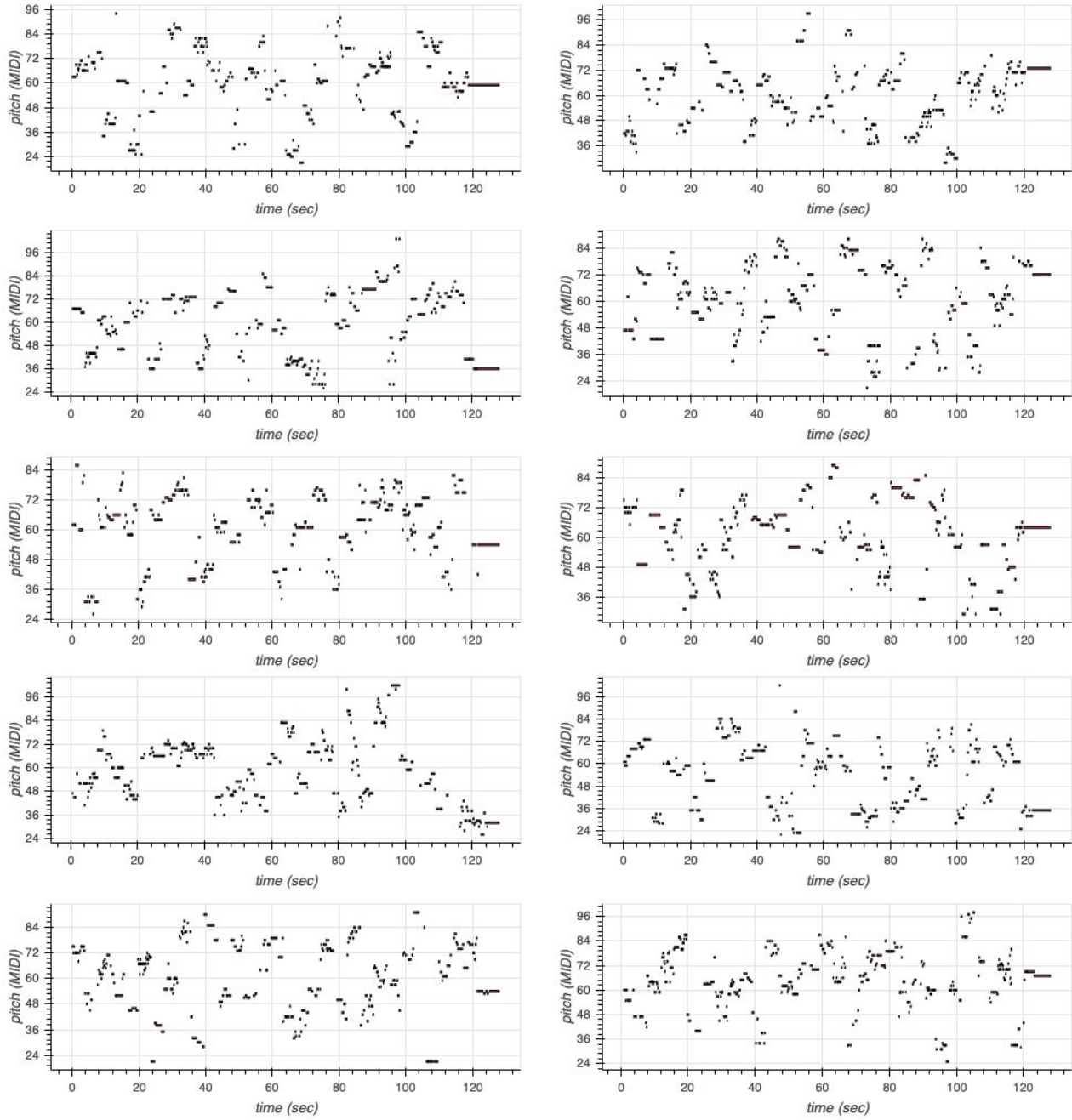


Figure 10. Additional piano rolls generated by sampling each latent embedding independently from the  $\mathcal{N}(0, I)$  MusicVAE prior.



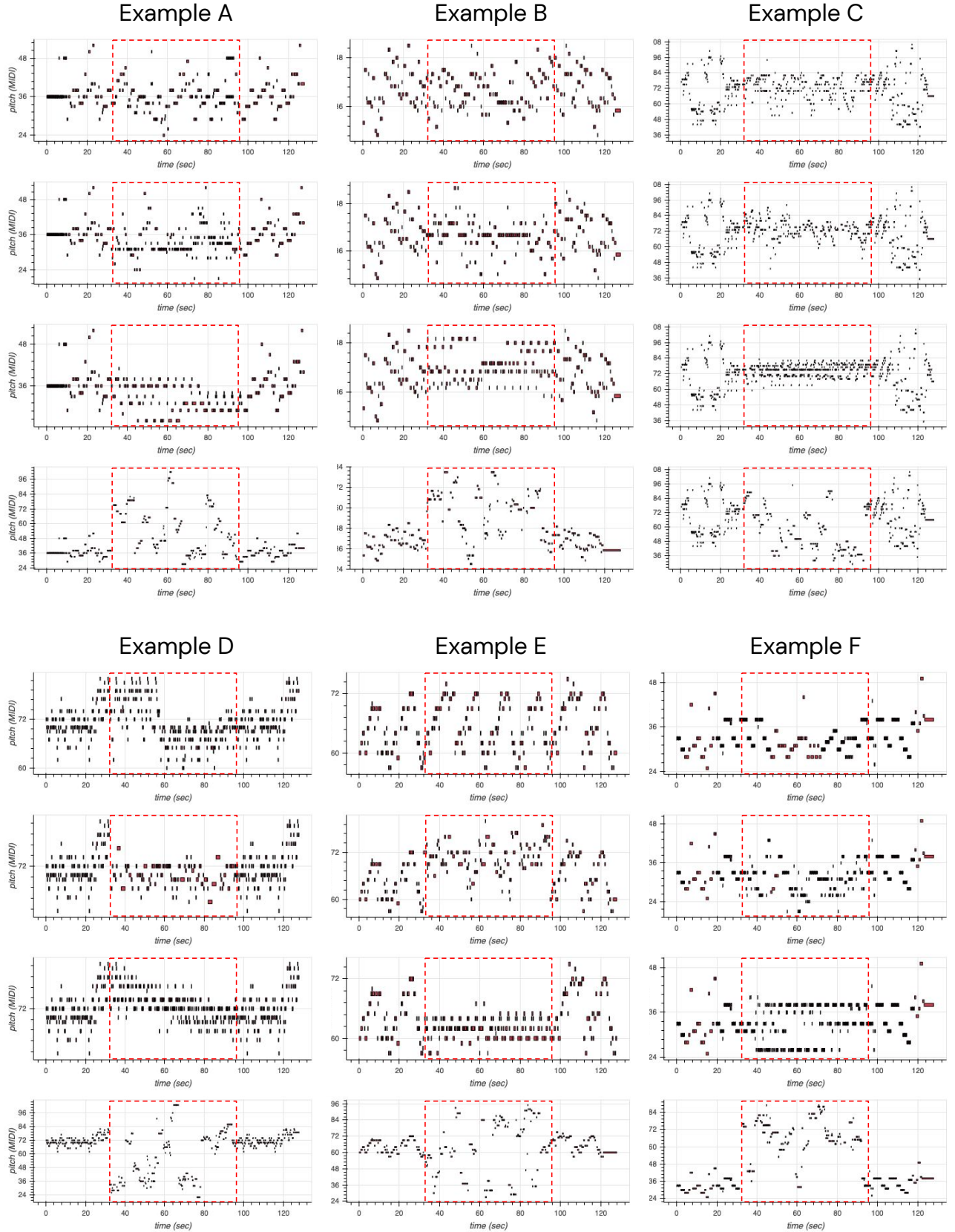


Figure 11. Additional piano rolls of infilling experiments. The first and last 256 melody tokens are held constant and the interior 512 tokens are filled in by the model (dashed red box). Original sample (first row), diffusion model (second row), interpolation (third row), sampling independently from the MusicVAE prior (fourth row).